CHEMISTRY AND TECHNOLOGY OF INORGANIC MATERIALS

ХИМИЯ И ТЕХНОЛОГИЯ НЕОРГАНИЧЕСКИХ МАТЕРИАЛОВ

ISSN 2686-7575 (Online)

https://doi.org/10.32362/2410-6593-2021-16-6-502-511

UDC 546.723 + 661.872.2

RESEARCH ARTICLE

Heterophase synthesis of cobalt ferrite

Elena E. Nikishina

MIREA – Russian Technological University (M.V. Lomonosov Institute of Fine Chemical Technologies), Moscow, 119571 Russia
@Corresponding author, e-mail: nikishina@mirea.ru

Abstract

Objectives. *The study aimed to develop new methods for the synthesis of cobalt ferrite ($CoFe_2O_4$), which is a precursor for the synthesis of $CoFe_2O_4$-based functional materials, as well as to study the physicochemical properties of the obtained phases.*
Methods. *Two methods were used for the synthesis of $CoFe_2O_4$: (1) heterophase interaction of hydrated iron oxide with cobalt(II, III) oxide and (2) heterophase interaction of hydrated iron oxide with an aqueous solution of cobalt(II) sulfate (C_{Co} = 0.147 mol/L, solid/liquid = 1:43). In both cases, the precursor was hydrated iron oxide (Fe_2O_3, 84.4 wt %), which was obtained by the heterophase interaction of iron(III) chloride with a concentrated ammonia solution (6.0–9.5 mol/L). The resulting intermediate products were subjected to thermal treatment at 750°C (synthesis **1**) and at 900°C (synthesis **2**) for 10–30 h in increments of 10 h. The synthesized phases and products of their thermolysis were studied by differential thermal analysis and differential thermogravimetry (DTA–DTG), X-ray diffraction analysis (XRDA), and granulometry.*
Results. *The hydrated iron oxide sample remained amorphous even up to the crystallization temperature of 445°C, which corresponds to the exothermic effect on the DTA curve. Further heating led to the α-modification of iron(III) oxide of the hexagonal system (a = b = 5.037 ± 0.002 Å; c = 13.74 ± 0.01 Å), which has an average particle size of 1.1 µm. XRDA results showed that a synthesis temperature of 750°C (synthesis **1**) and a heat treatment duration of 30 h were sufficient for the formation of a single-phase cobalt ferrite (a = 8.388 ± 0.002 Å) with an average particle diameter of 1.9 µm. For synthesis **2**, a higher temperature of 900°C was*

used because sample weight loss (about 12.5%) was observed in the temperature range of 720–810°C based on the DTA results, which was due to the removal of SO_2 *and* SO_3*. Moreover, when synthesis temperature and duration were at 900°C and 30 h, respectively,* $CoFe_2O_4$ *with a = 8.389 ± 0.002 Å was formed. The results of the granulometric analysis showed that particles of different diameters were formed. The smallest particle size (1.5 μm) of cobalt ferrite was obtained by the heterophase interaction of hydrated iron(III) oxide (*Fe_2O_3*, 84.4 wt %) with an aqueous solution of cobalt sulfate with* C_{Co} *= 0.147 mol/L.*

Conclusions. *Depending on the method used for the synthesis of cobalt ferrite, particles of different diameters are formed. The smallest particle size of cobalt ferrite was obtained from the heterophase interaction of hydrated iron(III) oxide with an aqueous solution of cobalt(II) sulfate.*

Keywords: *iron, cobalt, ferrite, oxides, thermal analysis, X-ray phase analysis, particle size analysis*

For citation: Nikishina E.E. Heterophase synthesis of cobalt ferrite. *Tonk. Khim. Tekhnol. = Fine Chem. Technol.* 2021;16(6):502–511 (Russ., Eng.). https://doi.org/10.32362/2410-6593-2021-16-6-502-511

НАУЧНАЯ СТАТЬЯ

Гетерофазный синтез феррита кобальта

Е.Е. Никишина

МИРЭА – Российский технологический университет (Институт тонких химических технологий им. М.В. Ломоносова), Москва, 119571 Россия
@Автор для переписки, e-mail: nikishina@mirea.ru

Аннотация

Цели. *Разработка новых методов синтеза феррита кобальта (*$CoFe_2O_4$*), являющегося предшественником для синтеза функциональных материалов на его основе, а также исследование физико-химических свойств полученных фаз.*

Методы. *Гидратированный оксид железа и феррит кобальта получали гетерофазным методом. Синтезированные фазы и продукты их термолиза изучали методами дифференциально-термического анализа и дифференциальной термогравиметрии (ДТА–ДТГ), рентгенофазового анализа (РФА) и гранулометрии.*

Результаты. *В статье изложены результаты двух методов синтеза феррита кобальта (*$CoFe_2O_4$*) и исследования полученных фаз. В обоих случаях в качестве предшественника выступал гидратированный оксид железа(III) с содержанием* Fe_2O_3 *– 84.4 мас. %, полученный гетерофазным взаимодействием хлорида железа(III) с концентрированным раствором аммиака (6.0–9.5 моль/л). Первый способ заключался во взаимодействии гидратированного оксида железа(III) с оксидом кобальта(II, III), второй – во взаимодействии гидратированного оксида железа(III) с водным раствором сульфата кобальта(II) с концентрацией* C_{Co} *= 0.147 моль/л (Т : Ж = 1 : 43). Получившиеся промежуточные продукты подвергали термической обработке при 750 °С (синтез* ***1****) и 900 °С (синтез* ***2****) в течение 10–30 ч с шагом 10 ч.*

Выводы. *Феррит кобальта ($CoFe_2O_4$) получен двумя способами. С использованием комплекса методов (РФА, ДТА–ДТГ, гранулометрии) исследованы физико-химические свойства синтезированных образцов. Установлено, что гидратированный оксида железа(III) вплоть до температуры кристаллизации (445 °C), соответствующей экзотермическому эффекту на кривой ДТА, остается рентгеноаморфным. Дальнейшее нагревание его приводит к образованию α-модификации оксида железа(III) гексагональной сингонии (a = b = 5.037 ± 0.002 Å; c = 13.74 ± 0.01 Å), средний размер частиц которой равен 1.1 мкм. Согласно данным РФА, в синтезе* ***1*** *при 750 °C и продолжительности термообработки 30 ч образуется однофазный феррит кобальта (a = 8.388 ± 0.002 Å) со средним диаметром частиц 1.9 мкм. В интервале температур 720–810 °C в образце наблюдается убыль массы (около 12.5%), связанная с удалением SO_2 и SO_3. Поэтому в синтезе* ***2*** *температуру нагревания увеличивали до 900 °C. Показано, что при 900 °C и продолжительности синтеза 30 ч также образуется феррит кобальта ($CoFe_2O_4$) (a = 8.389 ± 0.002 Å). Результаты гранулометрического анализа указывают на зависимость диаметра образующихся частиц от способа получения феррита кобальта. Наименьший размер частиц (1.5 мкм) обнаружен у феррита кобальта, полученного гетерофазным взаимодействием гидратированного оксида железа(III) (Fe_2O_3 – 84.4 мас. %) с водным раствором сульфата кобальта с концентрацией $C(Co^{2+})$ = 0.147 моль/л.*

Ключевые слова: *железо, кобальт, феррит, оксиды, термический анализ, рентгенофазовый анализ, гранулометрический анализ*

Для цитирования: Никишина Е.Е. Гетерофазный синтез феррита кобальта. *Тонкие химические технологии.* 2021;16(6):502–511. https://doi.org/10.32362/2410-6593-2021-16-6-502-511

INTRODUCTION

Due to their unique properties, spinel-structured ferrites are widely used in various fields of science and technology. This class of magnetic ceramics is used in various applications, such as information storage systems, magnetic fluids, gas sensors, catalysts, rechargeable lithium batteries, magnetic cores, microwave absorbers, medical diagnostics and therapy, wastewater treatment, and biosensors [1–7].

The ferrite formula can be represented as AB_2O_4. It has a spinel structure (Fig. 1), where the tetrahedral A-position is occupied by ions in the oxidation state of +2 (e.g., Mg^{2+}, Fe^{2+}, Ni^{2+}, Co^{2+}, and Mn^{2+}). The octahedral B-position is mainly occupied by Fe^{3+} ions, but they can be replaced by other ions in the oxidation state of +3 (e.g., Al^{3+}, Cr^{3+}). If the A-position is occupied by ions in the +3 oxidation state and the B-position is equally populated by ions in the +2 and +3 oxidation states, the spinel structure is called reversed [8, 9].

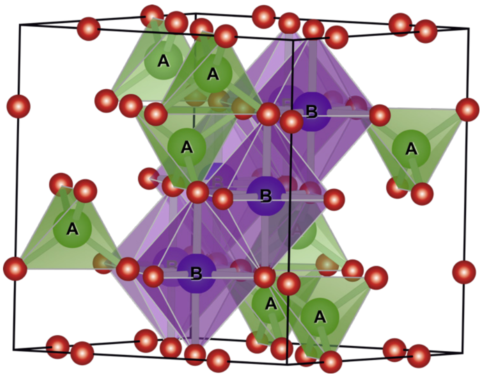

Fig. 1. Ferrite spinel structure [9].

One of the representatives of this class of materials is cobalt ferrite ($CoFe_2O_4$), a well-known magnetic hard material with a high coercive force associated with a small size of crystalline grains and strong magnetocrystalline anisotropy and moderate magnetization. It has an inverted spinel structure, where all or most of the Co^{2+} ions occupy an octahedral B-position and Fe^{3+} ions occupy both tetrahedral (A) and octahedral (B) positions.

These properties, along with high chemical stability, make it possible to use cobalt ferrite in various applications, such as medicine, catalysis, magnetic data carriers in audio and video cassettes, high-density digital recording discs, various sensors, recording devices, and solar cells [10–13].The purpose of this work was to develop methods for the synthesis of cobalt ferrite, which is a precursor for the synthesis of $CoFe_2O_4$-based functional materials, as well as to study the physicochemical properties of the obtained phases.

MATERIALS AND METHODS

Iron(III) chloride hexahydrate, which was used as the starting material in the study, cobalt(II, III) oxide, and cobalt sulfate were supplied by *Merck*, Germany, while aqueous ammonia was sourced from Himmed, Russia.

Hydrated iron(III) oxide was obtained by the heterophase interaction of iron(III) chloride with a concentrated solution of ammonia hydrate (6.0–9.5 mol/L).

Cobalt ferrite was synthesized using two heterophase synthesis methods.

*Synthesis **1***. Samples of hydrated iron(III) oxide and cobalt(II,III) oxide in the ratio of 1.5:1 were placed in a glass flask with a lapped stopper. The hydrated iron oxide to cobalt oxide ratio used was based on the oxide content of hydrated iron oxide and $CoFe_2O_4$. Distilled water was poured into the flask with the substance, and the flask containing the reaction mixture was shaken on a vibrating apparatus at roomtemperature (22 ± 2°C) for 10 h. The resulting suspension was transferred to a crucible and subjected to slow evaporation. Then, the intermediate product obtained was subjected to heat treatment at 750°C for 10–30 h in increments of 10 h.

*Synthesis **2***. A suspension of hydrated iron(III) oxide was placed in a glass flask with a lapped stopper, to which a solution of cobalt(II) sulfate with $C_{Co} = 0.147$ mol/L (solid/liquid = 1:43) was added. Then, the flask was shaken on a vibrating apparatus at room temperature for 10 h. The resulting suspension was transferred to a crucible and subjected to slow evaporation, and the intermediate product obtained was subjected to heat treatment at 900°C for 30 h in increments of 10 h.

The oxide content in hydrated iron(III) oxide was determined by gravimetric analysis.

Differential thermal analysis and differential thermogravimetry (DTA–DTG) of the samples was conducted on a Q-1500 D air derivatograph (*MOM*, Hungary) with simultaneous recording of four curves: differential (DTA), temperature (*T*), differential thermogravimetric (DTG), and integrated mass change (TG) curves using a hardware–software complex in LabVIEW 8.21 (*National Instruments*, USA). The temperature was measured with a platinum–platinum rhodium thermocouple (PP-1) with an error of ±5°C in the temperature range of 20–1000°C, using α-Al_2O_3 as a standard.

X-ray diffraction analysis (XRDA) was carried out on a D8 Advance diffractometer (*Bruker*, Germany) under SiK_α radiation with continuous rotation of the sample (1°/min, step-by-step $2\theta = 0.02°$, exposure 0.5 s) and modes in the angle range $2\theta = 5°$–$80°$. An ICDD card file was used for phase identification.

Granulometric analysis (determination of the particle size distribution function) was performed using a DelsaNano laser particle analyzer (*Beckman Coulter*, USA). Specific surface area and pore size were measured using a SA 3100 analyzer (*Beckman Coulter*, USA). Surface area was calculated from adsorption isotherms using the Brunauer–Emmett–Teller (BET) method. A nonporous sample ASX_1_4 (specific surface area according to BET was 4.18 m^2/g) GSO 9735_2010[1] (a set of standard samples of nanostructured aluminum oxide ASX_1) was used as a standard. The measurement range of the specific surface was 0.1–2000 m^2/g. The resolution of the pressure sensor was 0.0062 kPa. The limit of the permissible relative error of the analyzer when measuring the specific surface was ±5%. Preliminary degassing of the samples was carried out for 1 h at $t = 70°C$ and a pressure of 0.1 Pa.

Heat treatment of the samples was conducted in a TK-12.1250.N.1F laboratory furnace with a Thermomatic-N automatic temperature controller that has an error of ±1°C at nominal temperature.

RESULTS AND DISCUSSION

The heterophase synthesis of hydrated iron(III) oxide involves the interaction of solid ferric chloride with a concentrated ammonia solution (6.0–9.5 mol/L). The synthesis proceeded at a high rate at room temperature. Simultaneously, a well-filtered hydrated iron(III) oxide powder with a high content of Fe_2O_3 (84.4 wt %) was obtained, which was easily

---

[1] https://gsso.ru/wp-content/uploads/2016/08/catalog_gso_2020_3.pdf

washed off from impurities and retained a high reactivity. When obtaining hydrated iron(III) oxide, the prewashing operation is important, and it was conducted by the repeated treatment of the sediment with distilled water. Washing removes chloride ions in hydrated iron(III) oxide precipitate, thereby lowering its content to less than 0.05 wt %. Figure 2 shows the particle size distribution of hydrated iron(III) oxide. On the histogram (Fig. 2), there is a pronounced maximum corresponding to the maximum amount of powder particles with a size of 0.8–1.2 µm. Hence, it can be assumed that the hydrated iron(III) oxide was a relatively monodisperse powder. About 95% was accounted for by particles with a size of 0.7–2.0 µm.

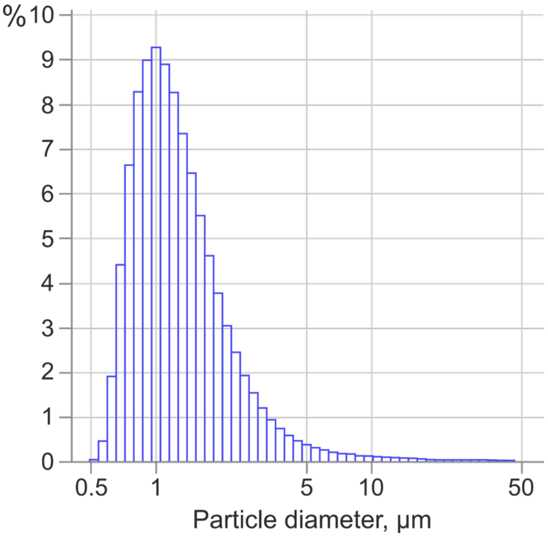

Fig. 2. Particle size distribution of hydrated iron(III) oxide.

Studies have shown that the average particle size is 1.1 µm. The specific surface area of hydrated iron(III) oxide measured by the BET method was 76.72 m^2/g.

Thermolysis of hydrated iron(III) oxide was studied in the temperature range of 20–1000°C. Figure 3 shows the results of the DTA. It was found that the loss of the bulk of water in hydrated iron(III) oxide at temperatures as high as 200°C corresponds to the endothermic effect on the DTA curve (Fig. 3). The resulting phase remains amorphous, which was confirmed by the results of XRDA. With a further increase in temperature, there are no other endoeffects that could indicate a stepwise dehydration. The exoeffect at 445°C corresponds to the transition from an amorphous state to a crystalline state. Further heating above the specified temperature is accompanied by the formation of crystalline oxide Fe_2O_3. Figure 4 shows the diffractogram of the thermolysis products of hydrated iron(III) oxide at 500°C. Obviously, at 500°C, a hexagonal α-modification of iron(III) oxide was formed. The parameters of the α-Fe_2O_3 lattice are as follows: $a = b = 5.037 \pm 0.002$ Å and $c = 13.74 \pm 0.01$ Å.

To establish the effect of the precursor on the phase composition of cobalt ferrite, two synthesis methods were conducted with hydrated iron(III) oxide acting as a precursor in both. Either cobalt oxide Co_3O_4 (synthesis **1**) was added to it, or an aqueous solution of cobalt(II) sulfate ($C_{Co} = 0.147$ mol/L, synthesis **2**).

Figures 5 and 6 show the results of the thermal analysis of the intermediate products obtained during syntheses after evaporation of suspensions.

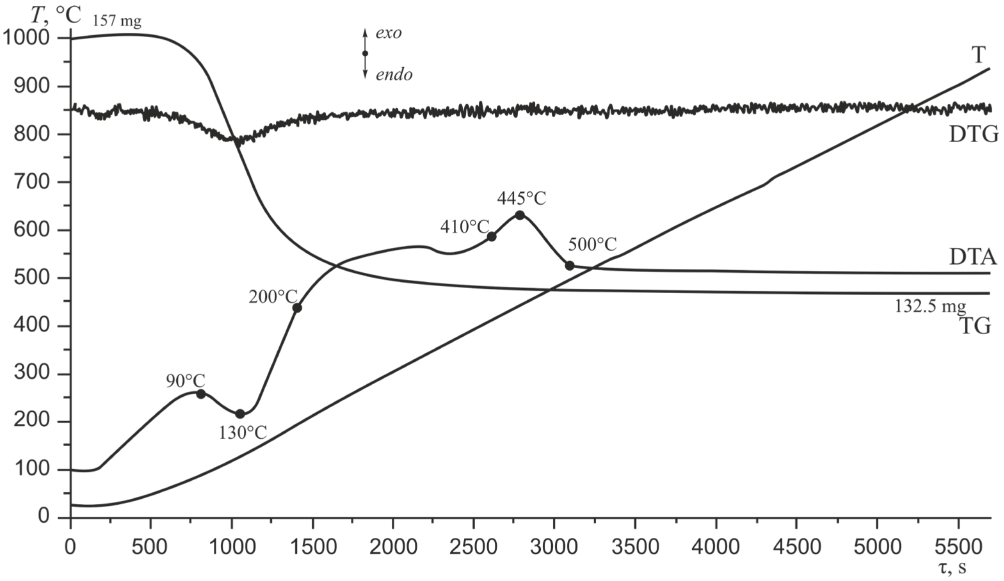

Fig. 3. Thermogravitogram of hydrated iron(III) oxide (Fe_2O_3, 84.4 wt %).

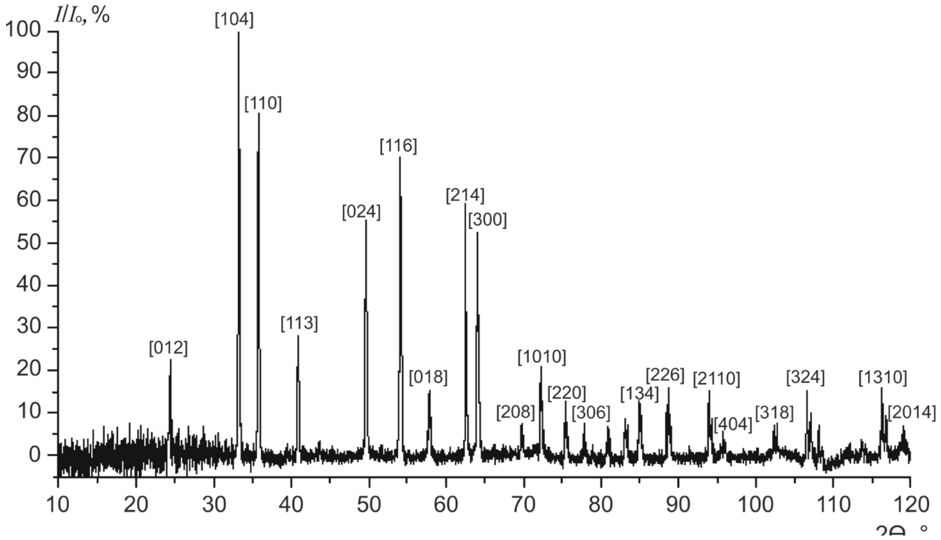

Fig. 4. X-ray diffraction pattern of the thermal decomposition product of hydrated iron(III) oxide, $T = 500°C$.

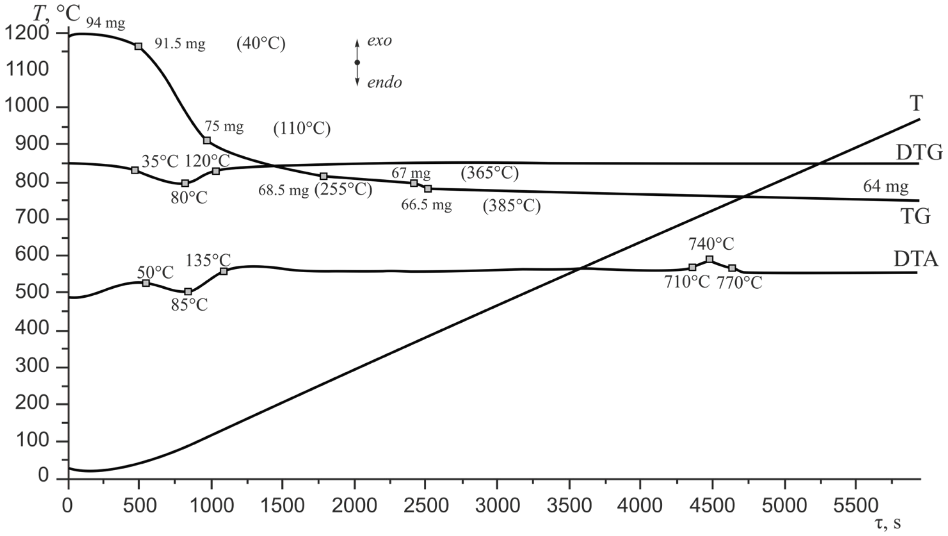

Fig. 5. Thermogravitogram of the intermediate product obtained by the interaction of hydrated iron(III) oxide with cobalt(II, III) oxide (synthesis **1**).

Thermogravitograms showed an endothermic effect associated with the dehydration processes (50–135°C, Fig. 5; 75–160°C and 275–330°C, Fig. 6) and with the removal of SO_2 and SO_3 (725–805°C and 805–870°C [15], Fig. 6). In both cases, there was no exothermic effect at 445°C that corresponds to the crystallization of individual hydrated iron(III) oxide. On the thermogravitogram of the intermediate product obtained by the interaction of hydrated iron(III) oxide with cobalt(II, III) oxide (Fig. 5), an exoeffect was observed at 710–770°C, which can be associated with the formation of a compound of a given composition, but the sample annealed at 710°C was amorphous.

The resulting intermediates were subjected to heat treatment. In the case of synthesis **1**, a temperature of 750°C was used, corresponding to the exothermic effect on the DTA curve (Fig. 5), and the synthesis duration was 10–30 h in increments of 10 h. In all cases, fine crystalline powder of $CoFe_2O_4$ (cubic syngony) was obtained, which is confirmed by the results of XRDA (ICDD 79-1744: $a = 8.390$ Å). However, in the case of 10-h annealing, the diffraction peaks of unreacted iron and cobalt oxides were observed on the diffractogram (Fig. 7). Annealing for 30 h turned out to be the most optimal—pronounced peaks of only one phase are present on the diffractogram, which is cubic ($CoFe_2O_4$, Fig. 8). The calculated lattice parameter of the synthesized cobalt ferrite is $a = 8.388 \pm 0.002$ Å.

In synthesis **2**, an annealing temperature of 900°C was selected. This is due to the fact that up to a temperature of 870°C, there was a decrease in

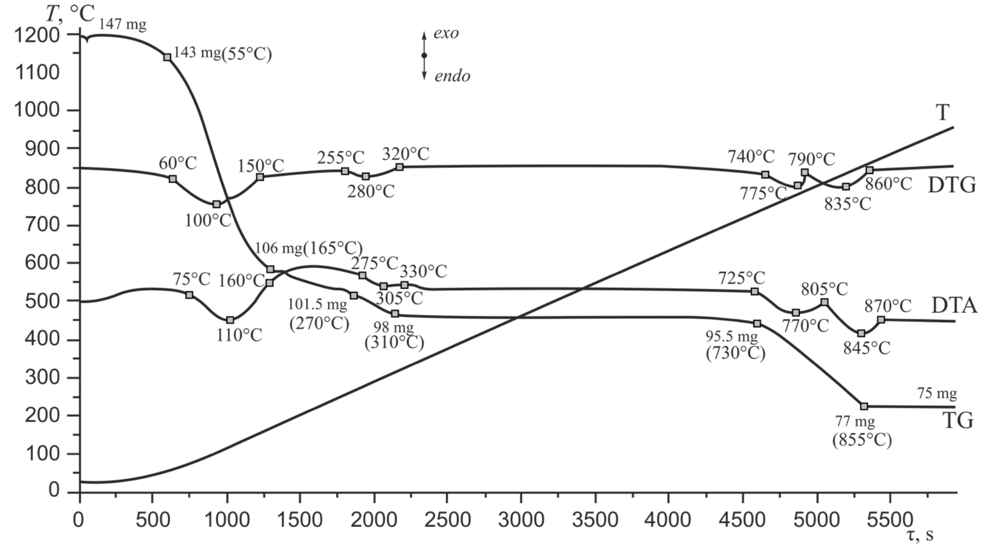

Fig. 6. Thermogravitogram of the intermediate product obtained by the interaction of hydrated iron(III) oxide with a solution of cobalt(II) sulfate (synthesis **2**).

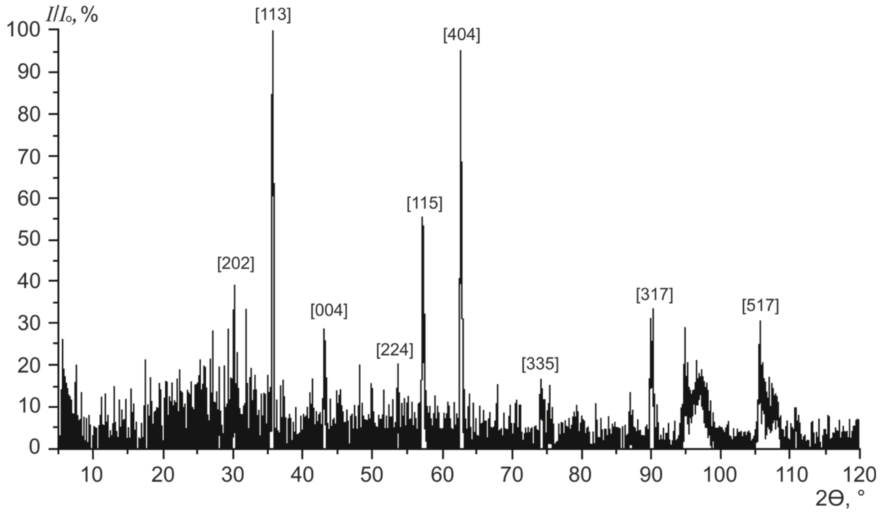

Fig. 7. X-ray diffraction pattern of cobalt ferrite synthesized at 750°C and annealed for 10 h (synthesis **1**).

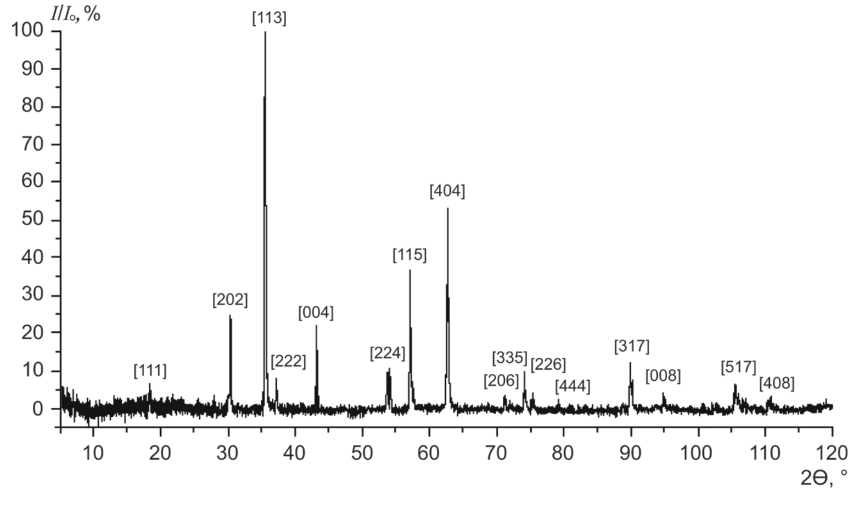

Fig. 8. X-ray diffraction pattern of cobalt ferrite synthesized at 750°C and annealed for 30 h (synthesis **1**).

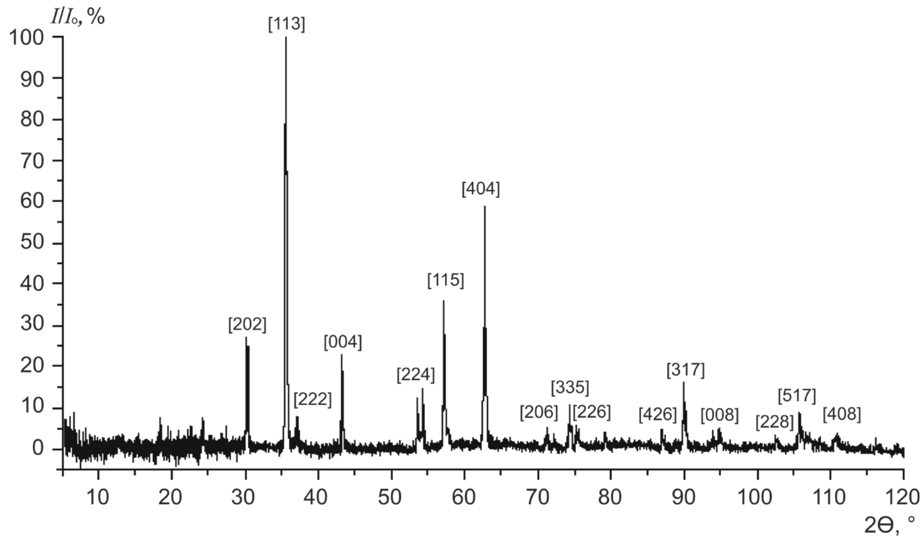

Fig. 9. X-ray diffraction pattern of cobalt ferrite synthesized at 900°C and annealed for 30 h (synthesis **2**).

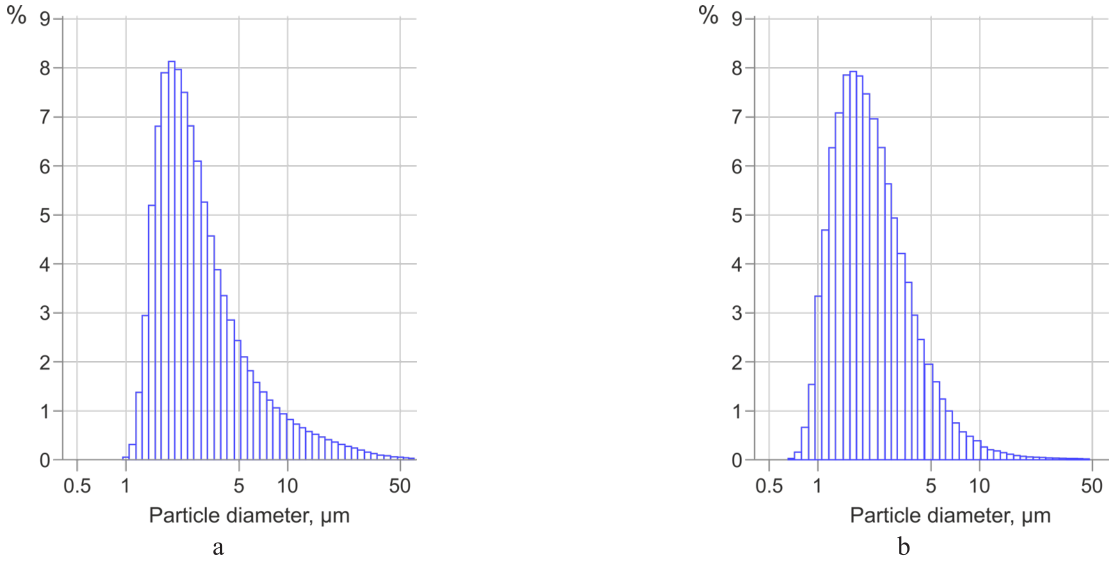

Fig. 10. Particle size distribution of cobalt ferrite: (a) synthesis **1**, 750°C, 30 h; (b) synthesis **2**, 900°C, 30 h.

sample mass (about 12.5%, Fig. 6). The duration of annealing was 30 h. Figure 9 shows the diffractogram of the resulting product. The lattice parameter of the synthesized cobalt ferrite is a = 8.389 ± 0.002 Å.

The influence of the choice of precursors on the size of cobalt ferrite particles has been studied. Figure 10a shows the size distribution of cobalt ferrite particles (synthesis **1**, 750°C, 30 h). On the histogram (Fig. 10a), there is a pronounced maximum corresponding to the maximum presence of powder particles with a size of 1.5–3.0 µm. The main fraction consisted of particles with a size of 1.0–5.0 µm (~85%) with an average diameter of 1.9 µm (for the initial hydrated iron(III) oxide, it was 1.1 µm).

Figure 10b shows the size distribution of cobalt ferrite particles (synthesis **2**, 900°C, 30 h). In this case, it is obvious from the histogram that a maximum number of cobalt ferrite powder particles have a size of 1.2–3.0 µm, and the average particle diameter was 1.5 µm.

As can be seen from the distributions, the smallest particles were formed in cobalt ferrite obtained by the heterophase interaction of hydrated iron(III) oxide (Fe_2O_3, 84.4 wt %) with an aqueous solution of cobalt(II) sulfate with C_{Co} = 0.147 mol/L.

CONCLUSIONS

$CoFe_2O_4$ was synthesized in two ways. The first method is the heterophase interaction of hydrated iron(III) oxide with cobalt(II, III) oxide with subsequent thermal treatment at 750°C for 30 h (synthesis **1**), and the second method is the heterophase interaction of hydrated iron(III) oxide

(Fe_2O_3, 84.4 wt %) with an aqueous solution of cobalt(II) sulfate (C_{Co} = 0.147 mol/L) with subsequent heat treatment at 900°C for 30 h (synthesis **2**).

Using various methods (XRDA, DTA–DTG, and granulometry), the physicochemical properties of the synthesized samples were investigated. The results of the studies on hydrated iron(III) oxide showed that up to the crystallization temperature of 445°C, which corresponds to the exothermic effect on the DTA curve, the sample remained amorphous. Further heating led to the α-modification of iron(III) oxide hexagonal syngony ($a = b = 5.037 \pm 0.002$ Å; $c = 13.74 \pm 0.01$ Å), which has an average particle size of 1.1 µm.

Using the XRD method, it was found that in the case of synthesis 1, a temperature of 750°C and a heat treatment for 30 h were sufficient to form a single-phase cobalt ferrite ($a = 8.388 \pm 0.002$ Å) with an average particle diameter of 1.9 µm. The temperature used in synthesis **2** was increased to 900°C due to a decrease in sample mass (about 12.5%) observed during synthesis in the temperature range of 720–810°C based on the results of differential thermal analysis. Loss in sample mass was due to the removal of SO_2 and SO_3. Using a synthesis temperature and a synthesis duration of 900°C and 30 h, respectively, $CoFe_2O_4$ with a = 8.389 ± 0.002 Å was formed.

Depending on the synthesis method, cobalt ferrite particles of different diameters were formed. The smallest particle size of cobalt ferrite (1.5 µm) was obtained by the heterophase interaction of hydrated iron(III) oxide (Fe_2O_3, 84.4 wt %) with an aqueous solution of cobalt(II) sulfate with C_{Co} = 0.147 mol/L.

Acknowledgments

This work was performed using the equipment of the Join Science and Training Center for Collective Use and supported by The Ministry of Education and Science of the Russian Federation.

Author's contribution

Elena E. Nikishina – conducting research, preparing a manuscript.

The author declares no conflicts of interest.

REFERENCES

1. Yan Z., Gao J., Li Y., Zhang M., Guo M. Hydrothermal synthesis and structure evolution of metal-doped magnesium ferrite from saprolite laterite. *RSC Advances.* 2015;5:92778–92787. https://doi.org/10.1039/C5RA17145H

2. Kefeni K.K., Mamba B.B., Msagati T.A.M. Application of spinel ferrite nanoparticles in water and wastewater treatment: A review. *Sep. Purif. Technol.* 2017 Nov;188:399–422. https://doi.org/10.1016/j.seppur.2017.07.015

3. Rashdan S.A., Hazeem L.J. Synthesis of spinel ferrites nanoparticles and investigating their effect on the growth of microalgae Picochlorum sp. *Arab J. Basic Appl. Sci.* 2020 Feb;27(1):134–141. https://doi.org/10.1080/25765299.2020.1733174

4. Amiri M., Salavati-Niasari M., Akbari A. Magnetic nanocarriers: Evolution of spinel ferrites for medical applications. *Adv. Colloid Interface Sci.* 2019 Mar;265:29–44. https://doi.org/10.1016/j.cis.2019.01.003

5. Vedrtnam A., Kalauni K., Dubey S., Kumar A. A comprehensive study on structure, properties, synthesis and characterization of ferrites. *AIMS Materials Science.* 2020;7(6):800–835. https://doi.org/10.3934/matersci.2020.6.800

6. Zhou J., Shu X., Wang Y., Ma J. *et al.* Enhanced Microwave Absorption Properties of (1-x)$CoFe_2O_4$/xCoFe Composites at Multiple Frequency Bands. *J. Magn. Magn. Mater.* 2020 Jun;493:165699–165708. https://doi.org/10.1016/j.jmmm.2019.165699

7. Bartunek V., Sedmidubsky D., Hube, S., Svecov, M., Ulbrich P., Jankovsky O. Synthesis and properties of nanosized stoichiometric cobalt ferrite spinel. *Materials.* 2018 Jul;11(7):1241–1251. https://doi.org/10.3390/ma11071241

8. Zhou Z., Zhang Y., Wang Z., Wei W., *et al.* Electronic structure studies of the spinel $CoFe_2O_4$ by X-ray photoelectron spectroscopy. *Appl. Surf. Sci.* 2008 Aug;254(21):6972–6975. https://doi.org/10.1016/j.apsusc.2008.05.067

9. Das D., Biswas R., Ghosh S. Systematic analysis of structural and magnetic properties of spinel CoB_2O_4 (B=Cr, Mn and Fe) compounds from their electronic structures. *J. Phys.: Condens. Matter.* 2016 Nov;28(44):446001–446010. https://doi.org/10.1088/0953-8984/28/44/446001

10. Swatsitang E., Phokha S., Hunpratub S., Usher B., Bootchanont A., Maensiri S., *et al.* Characterization and magnetic properties of cobalt ferrite nanoparticles. *J. Alloys Compd.* 2016 Apr;664:792–797. https://doi.org/10.1016/j.jallcom.2015.12.230

11. Kazemi M., Ghobadi M., Mirzaie A. Based on: Cobalt ferrite nanoparticles ($CoFe_2O_4$ MNPs) as catalyst and support: Magnetically recoverable nano-catalysts in organic synthesis. *Nanotechnol. Rev.* 2017 Jan;7(1):1–50. https://doi.org/10.1515/ntrev-2017-0138

12. Srinivasan S.Y., Paknikar K.M., Bodas D., Gajbhiye V. Applications of cobalt ferrite nanoparticles in biomedical nanotechnology. Nanomedicin. 2018 Jun;13(10):1221–1238. https://doi.org/10.2217/nnm-2017-0379

13. Chagas C.A., de Souza E.F., de Carvalho M.C.N.A., Martins R.L., Schmal M. Cobalt ferrite nanoparticles for the preferential oxidation of CO. *Appl. Catal. A-Gen.* 2016;519C:139–145. https://doi.org/10.1016/j.apcata.2016.03.024

14. Tatarchuk T., Bououdina M., Vijaya J.J., Kennedy L.J. Spinel Ferrite Nanoparticles: Synthesis, Crystal Structure, Properties, and Perspective Applications. In: *International Conference on Nanotechnology and Nanomaterials. NANO 2016: Nanophysics, Nanomaterials, Interface Studies, and Applications.* 2016 Aug:305–325. https://doi.org/10.1007/978-3-319-56422-7_22

15. Mu J., Perimutte D.D. Thermal Decomposition of Inorganic Sulfates and Their Hydrates. *Ind. Eng. Chem. Process Des. Dev.* 1981 Oct;20(4):640–646. https://doi.org/10.1021/i200015a010

About the author:

Elena E. Nikishina, Assistant Professor, Department of Chemistry and Technology Rare Elements, M.V. Lomonosov Institute of Fine Chemical Technologies, MIREA – Russian Technological University (86, Vernadskogo pr., Moscow, 119571, Russia). E-mail: nikishina@mirea.ru. Scopus Author ID 6602839662, ResearherID O-7115-2014, http://orcid.org/0000-0003-3579-2194

Об авторе:

Никишина Елена Евгеньевна, доцент кафедры химии и технологии редких элементов Института тонких химических технологий им. М.В. Ломоносова ФГБОУ ВО «МИРЭА – Российский технологический университет» (119571, Россия, Москва, пр-т Вернадского, д. 86). E-mail: nikishina@mirea.ru. Scopus Author ID 6602839662, ResearherID O-7115-2014, http://orcid.org/0000-0003-3579-2194

The article was submitted: October 05, 2021; approved after reviewing: October 26, 2021; accepted for publication: November 26, 2021.

Translated from Russian into English by N. Isaeva
Edited for English language and spelling by Enago, an editing brand of Crimson Interactive Inc.